Eur. Phys. J. B **16**, 67–72 (2000)

THE EUROPEAN PHYSICAL JOURNAL B

EDP Sciences

Field-induced phase transitions and giant magnetoresistance in Dy_3Co single crystals

N.V. Baranov[1], E. Bauer[2,a], R. Hauser[2], A. Galatanu[3], Y. Aoki[4], and H. Sato[4]

[1] Inst. of Phys. and Applied Math., Ural State Univ., 620083 Ekaterinburg, Russia
[2] Institut für Experimentalphysik, Technische Universität Wien, 1040 Wien, Austria
[3] National Institute for Materials Physics, 76900 Bucharest-Magurele, Romania
[4] Department of Physics, Tokyo Metropolitan University, Tokyo 192-0397, Japan

Received 15 July 1999 and Received in final form 6 December 1999

Abstract. Electrical resistivity and calorimetric measurements on Dy_3Co show that below the Néel temperature ($T_N = 44$ K) the non-collinear antiferromagnetic structure exhibits field-induced magnetic phase transitions of a first-order type along all principal axes, accompanied by a strongly anisotropic giant magnetoresistance and by a change of the Sommerfeld coefficient of the specific heat. Quantum tunnelling of the magnetization appears to be possible for $T < 0.6$ K.

PACS. 72.15.Eb Electrical and thermal conduction in crystalline metals and alloys – 75.30.Kz Magnetic phase boundaries (including magnetic transitions, metamagnetism, etc.) – 75.40.-s Critical-point effects, specific heats, short-range order

1 Introduction

During the last few years, increasing interest was devoted to field-induced magnetic phase transitions. In strongly anisotropic materials, such first-order phase transitions (FOMPTs) are characterised by so-called spin-flip processes [1] and are accompanied by dramatic changes of structural, electrical and magnetic properties [2]. One of the most striking features deduced at these FOMPTs are huge changes of the resistivity, matching that of giant magnetoresistance systems (GMR) based on artificial multilayers. Moreover, the Sommerfeld coefficient of the specific heat at such a FOMPT varies dramatically, indicating substantial changes of the density of states at the Fermi energy.

The series RE_3T with RE = rare earth and T = Ni, Co, exhibit the largest RE content among RE compounds and crystallise in the Fe_3C type of structure (space group: Pnma). A rich variety of temperature and field induced magnetic states are already known [3]. Dy_3Co orders antiferromagnetically below $T_{N_1} = 44$ K, but below $T_{N_2} = 32$ K a reorientation of this structure takes place. For $T < T_{N_1}$, field dependent measurements evidence metamagnetic behaviour which can be associated with a complex non-collinear magnetic structure [4]. Strong crystalline electric fields due to the low symmetry of this compound give rise to easy magnetisation directions which differ from one Dy atom to another. The direction of the magnetic moments along these easy axes is determined by exchange interactions. According to a preliminary neutron diffraction study, the magnetic structure of Dy_3Co at low temperatures has a period doubled along the a- and c-axes [4].

In this study we present magnetoresistance measurements down to 0.3 K and fields up to 12 T. The thus observed results allow us to analyse the temperature dependent width ΔH of the hysteresis loops of the FOMPTs. At the lowest temperatures, significant deviations of $\Delta H(T)$ from a thermal activated behaviour become obvious. The appearance of GMR at the FOMPTs is accounted for in terms of energy gaps on superzone boundaries, finding some corroboration by the field dependent changes of the γ value of the specific heat. In the vicinity of a FOMPT, an "intermediate" state may be observed in which properties of the different phases coexist. The overall behaviour of the magnetoresistance of Dy_3Co data will be discussed in terms of conduction electron scattering with magnetic moments, interphase boundaries, electron-magnon interaction, as well as s-electron transfer from one phase to another overcoming a potential barrier.

Dy_3Co single crystals were prepared by arc melting in He atmosphere and subsequently by remelting the ingots in a resistance furnace with a higher temperature gradient near the peritectic point. The ingots were annealed at 900 K for 3 days. The quality of the single crystals was checked by X-ray Laue pattern obtained from different surfaces of the samples. No extra reflections from other grains were detected. Some traces of foreign phases (less than 3%) were found by metallographic sample preparation.

[a] e-mail: bauer@xphys.tuwien.ac.at

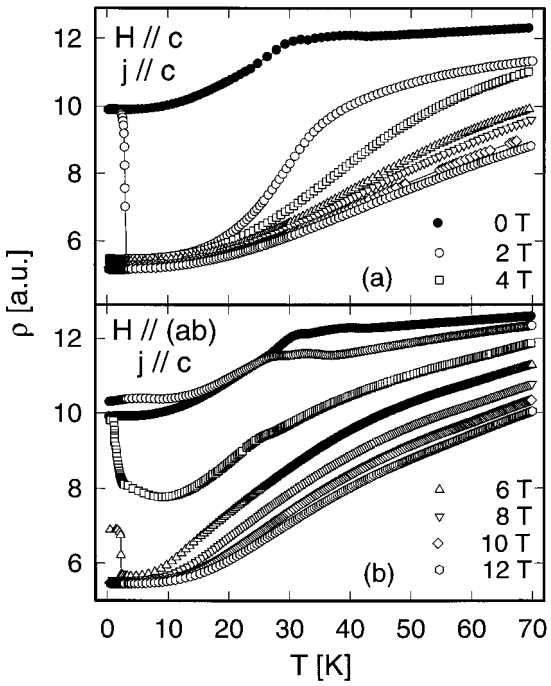

Fig. 1. Temperature and field dependence of the electrical resistivity of Dy_3Co single crystals, (a): $H \parallel ab$ and $j \parallel c$, and (b): $H \parallel ab$ and $j \parallel c$.

The isothermal magnetisation of Dy_3Co was measured on a single crystal of about $2 \times 2 \times 2$ mm^3 in fields up to 7 T using a vibrating sample magnetometer. Magnetoresistance measurements were performed on a bar-shaped sample with dimensions of about $1 \times 1 \times 2$ mm^3 in fields up to 12 T employing a common four-probe d.c. technique. A ^{3}He cryostat was used to obtain temperatures down to 300 mK. The heat capacity was studied by an adiabatic method in the temperature range from 0.1 up to 7 K in fields up to 8 T applied along the c-axis of a single crystal with a mass of about 200 mg.

2 Results and discussion

Figure 1a displays the electrical resistivity $\rho(T)$ of Dy_3Co measured at various values of applied magnetic fields ($H \parallel c$, $j \parallel c$). At $\mu_0 H = 0$, a phase transition into an antiferromagnetic state below $T_{N_1} \approx 44$ K is obvious from distinct changes in $\rho(T)$, in agreement with reference [5]. Below 30 K $\rho(T)$ decreases substantially, marking the reorientation of the magnetic structure at T_{N_2}. After applying a field of 1.5 T at the lowest temperatures (≈ 300 mK), the resistivity changes dramatically at $T_\mathrm{m} \approx 2.9$ K. The shape of $\rho(T)$ at this field indicates that either both transitions at T_{N_1} and T_{N_2} merge together or one of the transitions is suppressed by the magnetic field. If the field strength is further increased, T_m becomes reduced and eventually vanishes at $\mu_0 H \approx 3.5$ T. Measurements above this field exhibit no anomalous temperature dependencies but the magnetoresistance, $\Delta\rho/\rho = (\rho(H) - \rho(0))/\rho(H)$, remains large. Indications of an antiferromagnetic transition are no longer resolved. On the other hand, the magnetic transition is well resolved for fields ≤ 1 T; however, the field influence on the ordering temperature is insignificant (not shown here). In that case a small positive magnetoresistance is deduced ($\approx 1\%$).

Figure 1b presents the field and temperature dependence of ρ for $H \parallel ab$ and $j \parallel c$. On the contrary to the previous case, Dy_3Co enters possibly an intermediate state for fields around 4 T. Therefore, at $T \approx 1.1$ K and $T \approx 1.9$ K step-like changes occur in $\rho(T)$ for fields of 4 T and 6 T, respectively. In both cases as well as in the previous one, field cooling does not reproduce these sudden changes. For an applied field of 2 T a positive magnetoresistance is obtained up to 25 K, which may be associated with the particular antiferromagnetic spin configuration, but no field induced transition is resolved. Note, for $H \parallel c$ only 1.5 T are sufficient to induce such a phase transition. Indications for an antiferromagnetic transition, however, can be found in fields of 4 T at $T \approx 29$ K, while a spin reorientation occurs up to 2 T at $T_{N_2} \approx 26$ K.

Figures 2a, 3 and 4 show isothermal magnetoresistance measurements at various temperatures for different field – and current orientations. For the purpose of comparison, the previously reported magnetisation curves at $T = 4.2$ K are added in Figure 2b [4]. The magnetoresistance curves measured along all principal crystallographic directions of Dy_3Co (Fig. 2a) reveal a step-like behaviour, in agreement with the isothermal magnetisation data. This correlation between the magnetization and magnetoresistance curves indicates that the change of the electrical resistivity in Dy_3Co under applied magnetic fields is driven by a rearrangement of the initial antiferromagnetic structure. As was shown in reference [4], the magnetic structure of Dy_3Co at $T = 4.2$ K can be described by two wave vectors $\mathbf{k} = 0$ and $\mathbf{k} = 2\pi(1/2a, 0, 1/2c)$. However, the particular arrangement of the magnetic moments of the 48 Dy atoms in the magnetic unit cell is not determined yet. When extrapolating the isothermal magnetization from above the critical fields to $\mu_0 H \to 0$, the projections of the Dy magnetic moment onto the a-, b- and c-axes result to 6.0 μ_B, 4.5 μ_B and 6.3 μ_B, respectively. These values together sum up to a total magnetic moment of 9.8 μ_B, close to $gJ = 10$ μ_B for the free Dy^{3+} ion. The magnetization data indicate that the magnetic field applied along the main crystallographic directions induces the non-collinear magnetic structures *via* spin-flip processes. These field-induced structures are characterized by a ferromagnetic alignment of the projections of the Dy magnetic moment onto the field directions and by an antiferromagnetic alignment of the projections in the plane perpendicular to H and may be specified by an average angle between the Dy magnetic moments and the corresponding crystallographic direction: 53° for the a-axis, 63° for the b-axis and 51° for c-axis [4].

The magnetoresistance $\Delta\rho/\rho$ at low temperatures and $H \perp c$ is characterized by FOMPTs at about 4 and 6 T (Fig. 3). On the contrary, only one FOMPT occurs in the case of $H \parallel c$ (Fig. 4). The transition field of 2.9 T

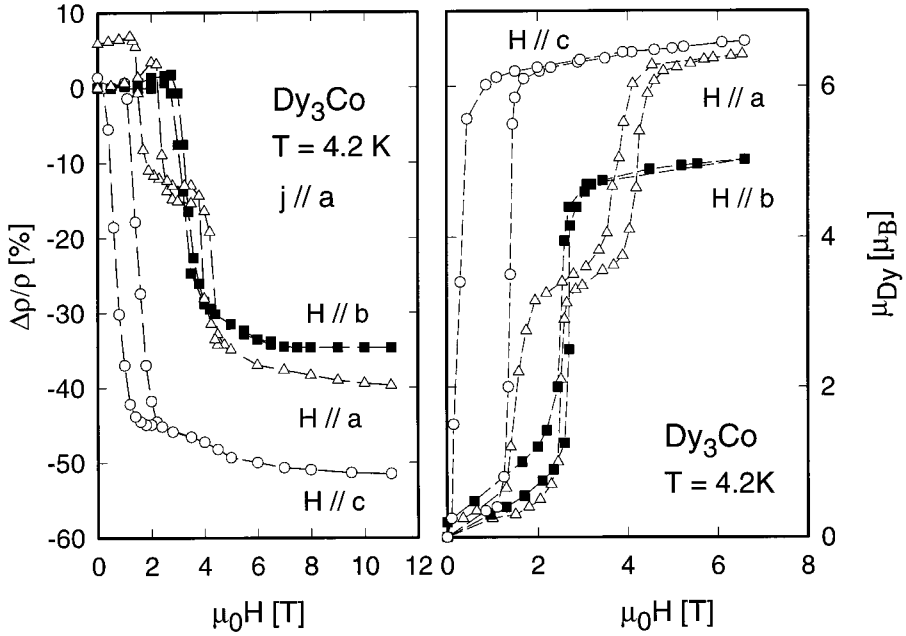

Fig. 2. (a) Magnetoresistance curves measured at $T = 4.2$ K along the principal crystallographic direction of Dy_3Co with the current direction $j \parallel a$. (b) Isothermal magnetisation curves at $T = 4.2$ K for the principal crystallographic directions of Dy_3Co.

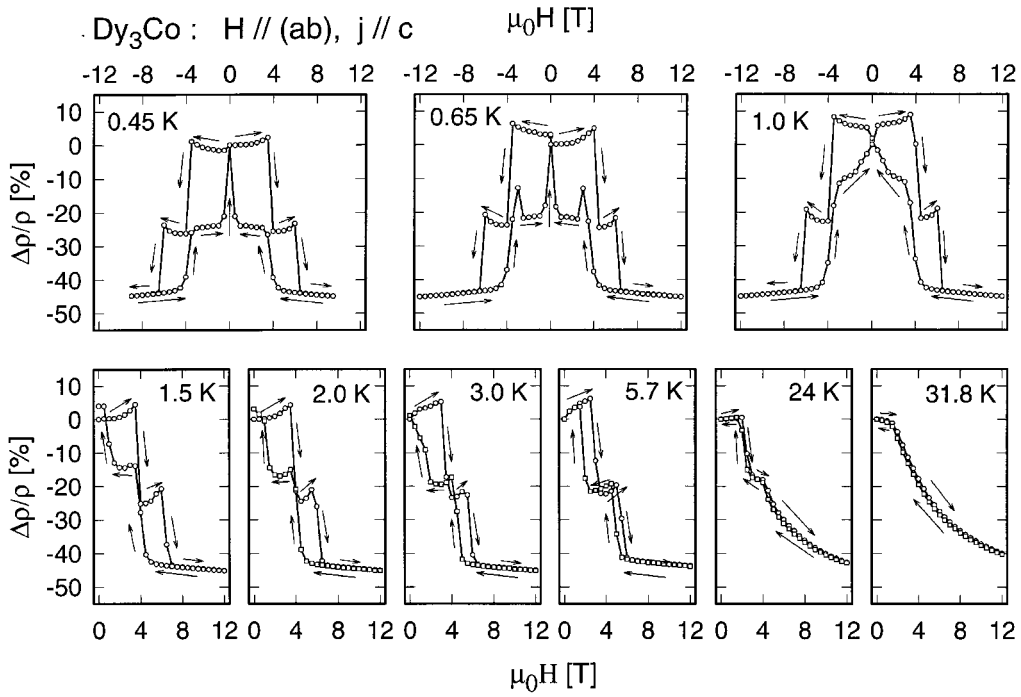

Fig. 3. Isothermal magnetoresistance measurements of Dy_3Co single crystals at different temperatures with $j \parallel c$ and $H \perp c$.

at 0.5 K decreases to about 1.75 T at 5 K. For fields larger than the critical one, $\Delta\rho/\rho$ is almost constant since the FOMPTs cause a ferromagnetic alignment of the Dy moment projections. Note that the values of the magnetoresistance in the field-induced ferromagnetic states are different for the different field directions as is obvious from Figure 2a. The absolute value of $\Delta\rho/\rho$ is larger for $H \parallel c$ where the projection of the Dy magnetic moment is also larger, in comparison with projections onto the b- and a-axes. This remarkable anisotropy of the magnetoresistance in Dy_3Co cannot simply be accounted for in terms of the anisotropy of the Fermi surface or of the contribution due to the Lorentz force since the isostructural compound Gd_3Co does not exhibit such an anisotropic field-induced ferromagnetic state [12]. By decreasing the applied field, hysteresis is observed which decreases with increasing

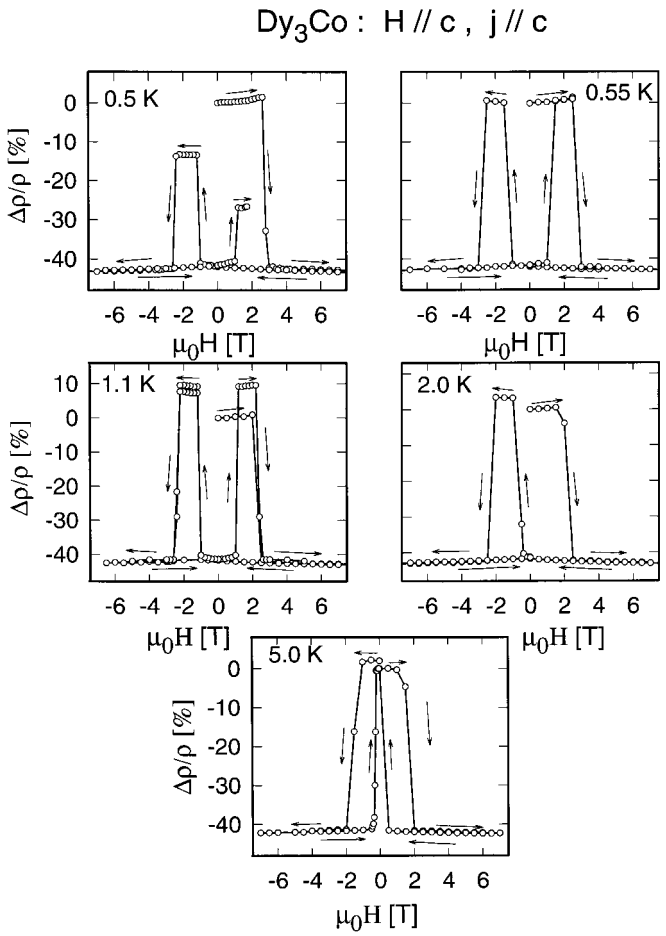

Fig. 4. Isothermal magnetoresistance measurements of Dy_3Co single crystals at different temperatures with $j \parallel c$ and $H \parallel c$.

temperatures. Eventually, the FOMPT vanishes and in the paramagnetic temperature range the magnetoresistance decreases smoothly; however even at 70 K, $\Delta\rho/\rho$ is as large as 20% for a field of 12 T.

In order to account for these substantial changes of the magnetoresistance at the field induced ferromagnetic transition, superzone boundary effects on the Fermi surface may be considered. Based on the semi-classical Boltzmann equation, the electrical resistivity is expressed as [6]

$$1/\hat{\rho} \equiv \hat{\sigma} = \frac{e^2}{8\pi^3\hbar} \sum_s \int \tau_s(\mathbf{v}_s)^2 \frac{\mathrm{d}S_\mathrm{F}}{|\mathbf{v}_s|}, \qquad (1)$$

where both the resistivity $\hat{\rho}$ and the conductivity $\hat{\sigma}$ are tensors. τ_s is the relaxation time and $\mathbf{v}_s$ the velocity of conduction electrons. The integral has to be taken over a constant energy surface in k-space with energy E_F. Superzone boundary effects are characterized by the vanishing of some parts of the Fermi surface near to the antiferromagnetic zone boundaries owing to the AF superzone gap formation [7]. According to equation (1), the conductivity of the AF phase is diminished, hence the resistivity is larger, as confirmed experimentally. Moreover, the electron velocity $\mathbf{v}_s$ may change between the ferro – and the antiferromagnetic phase. In general, the Fermi velocity

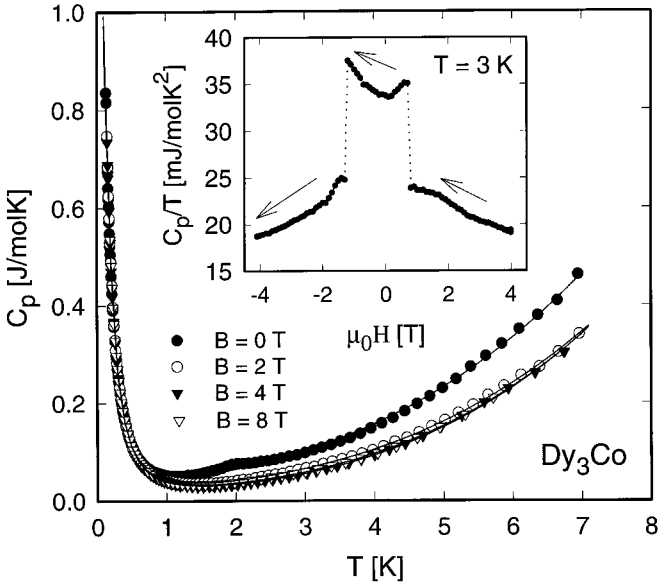

Fig. 5. Temperature dependent specific heat C_p of Dy_3Co. The solid lines are least squares fits according to equation 3. The inset shows the field dependence of C_p/T of Dy_3Co measured at $T = 3$ K.

is smaller in the AF phase, which then can be considered as a second mechanism to increase the resistivity. Superzone boundary effects revealing giant magnetoresistance values have already been found in a couple of compounds like UNiGa [8] $SmMn_2Ge_2$ [9] or FeRh [10].

Figure 5 shows low temperature measurements of the heat capacity C_p of Dy_3Co at various applied magnetic fields. In the inset, isothermal measurements of C_p/T at $T = 3$ K for fields from 4 T to −4 T are displayed, reflecting clearly the FOMPTs, already observed by the resistivity measurements. The change of γ ($= C_p/T$ for $T \to 0$) at the FOMPT is about 31%. Again, we assume that the decrease of γ, when proceeding from the AF to the F phase, is related to superzone boundary effects. Neglecting many-body mass-enhancement, the electronic contribution to the specific heat follows from [11]

$$\gamma = \frac{1}{8\pi^3\hbar} \frac{\pi^2 k_\mathrm{B}^2}{3} \sum_s \int \frac{\mathrm{d}S_\mathrm{F}}{|\mathbf{v}_s|}. \qquad (2)$$

Equation (2) depends again on changes of the Fermi surface and on the electron velocity. However, as inferred from the resistivity study, the Fermi surface decreases in the AF phase, thus, according to equation (2), γ should be smaller there, in contradiction to the experimental results. We therefore have to assume that the Fermi velocity is more drastically reduced in the AF phase, which outweighs in this case the diminishing of the Fermi surface due to superzone boundary effects. Note that spin fluctuations, generally present in rare earth–cobalt compounds, are supposed to be the origin of the slightly enhanced γ value of the specific heat of Dy_3Co ($\gamma \approx 25$ mJ/mol K^2 at $\mu_0 H = 0$ T). This contribution may be also changed at the AF–F transition. However, at higher magnetic fields, spin fluctuations become suppressed, hence γ reduces further.

Table 1. Parameters deduced from a fit of equation 3 to the heat capacity data of Dy_3Co.

	A [J K/mol]	B [J K^2/mol]	γ [J/(mol K^2)]	δ [J/(mol K^4)]
0 T	0.0283	−0.00184	0.0255	0.00083
2 T	0.0299	−0.00204	0.0144	0.00071
4 T	0.0299	−0.0020	0.010	0.00078
8 T	0.0304	−0.0021	0.0116	0.00075

The temperature dependent specific heat is characterized by an extremely large upturn for temperatures $T < 1$ K. In order to analyse the origin of this behaviour, the following model is used:

$$C_p = A/T^2 + B/T^3 + \gamma T + \delta T^3, \qquad (3)$$

where $(A/T^2 + B/T^3)$ represents a nuclear Schottky contribution and γT is the usual electronic contribution. The term B/T^3 does not vanish when quadrupolar effects exist. δT^3 accounts for the lattice and the magnetic contribution to the specific heat. This is expected to be justified since AF spin waves, well below the ordering temperature, yield $C_{\mathrm{mag}} \propto T^3$. The solid lines in Figure 5 represent least squares fits of equation (3) to the data. Excellent agreement is obtained and the thus deduced parameters A, B, γ and δ are collected in Table 1. Roughly around 2 K, the zero field measurement exhibits a slight anomaly, presumably due to magnetic impurity phases, which becomes totally suppressed already in fields of 2 T. Such a "hump" was also observed from a calorimetric study on pure Dy metal and was associated with dysprosium oxide impurities in the samples [13].

Various features are obvious from the present data: i) in the vicinity of each FOMPT and at increasing fields, a slight upturn of $\Delta\rho/\rho$ is observed. With increasing fields the FOMPTs are in general very sharp, while at decreasing fields they are slightly broader. Moreover, Cp/T exhibits a similar characteristic on approaching the critical field (compare inset, Fig. 5). A possible origin of such an enhancement may date from thermally activated processes of nucleation of the new magnetic phase in the vicinity of the FOMPT. In this case, however, the peak effect is expected to have comparable behaviour regardless of the field directions (compare Figs. 3 and 4). The strong structural and magnetic anisotropy of Dy_3Co and a difference in the exchange interaction in different magnetic phases can give rise to a potential barrier at the boundary between such phases [2]. Hence, a peak effect in the magnetoresistivity can be generated for increasing and decreasing fields the same as the one observed at $T = 0.65$ K (Fig. 3). Besides, Yamada and Takada [14] proposed such an enhancement of the magnetoresistance very near to a FOMPT due to significantly growing spin fluctuations. As a result, conduction electron scattering increases, too. ii) Below 3 K the application of a magnetic field creates remanent magnetization which strongly depends on the sample history, while above that temperature the magnetization process seems to be independent of the sample history. iii) For $H \parallel c$ the magnetoresistance shows a sharp transition at lower temperatures and the induced ferromagnetic state is persistent on decreasing and changing the external field direction. At $T = 0.4$ K an opposite field of 1.1 T was required to suppress the induced state. This field decreases steadily with growing temperatures and eventually becomes zero at about 4.1 K. A persistent ferromagnetic state was obtained at 0.4 K and also preserved after the field removal up to about 4 K.

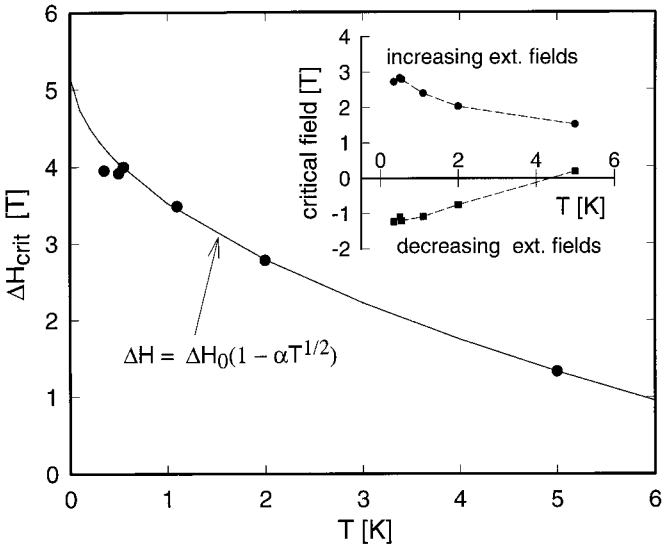

Fig. 6. Temperature dependence of the hysteresis loop width of the critical field of Dy_3Co. The solid line is a least squares fit according to equation (4). The inset shows the respective critical field values on increasing and decreasing fields.

The temperature dependent width of the hysteresis loop ($H \parallel c$) is analysed in Figure 6, defined from the critical fields where the FOMPTs occur with increasing and decreasing magnetic fields (inset, Fig. 6). For $T > 0.6$ K, the temperature dependent change of the width of the hysteresis loops ΔH can be accounted for by the following empirical expression:

$$\Delta H(T) = \Delta H_0(1 - \alpha T^{1/2}), \qquad (4)$$

where ΔH_0 and α are adjustable parameters. Equation (4) is derived from an approximation of a function obtained by Egami [15] used for the modelling of thermal activated domain wall displacement processes. A least squares fit of equation (4) to the data (solid line, Fig. 6) reveals $\Delta H_0 = 5.3$ T and $\alpha = 0.035$ $K^{-1/2}$. At lower temperatures, however, there is clear evidence that the activation type behaviour no longer holds, rather the domain wall

motion is possibly determined by a quantum tunnelling of the magnetization.

3 Summary

The investigations carried out on Dy_3Co characterize this binary compound as an example where superzone boundary effects are responsible for a giant magnetoresistance observed at low temperatures near to a field induced ferromagnetic state. These superzone boundary effects are corroborated in a similar manner by field dependent resistivity results as well as by field dependent heat capacity measurements.

The anisotropic magnetoresistance observed reflects the highly anisotropic non-collinear magnetic structure of Dy_3Co. Various reasons can be made responsible: i) anisotropy of the Fermi surface, ii) anisotropy of the energy gap on superzone boundaries and iii) anisotropic scattering of s-electrons by the quadrupolar moment of the $4f$-electron shell. As was demonstrated for pure rare earth metals, and in particular for Dy at low temperatures, the latter mechanism can give rise to anisotropy values of the order of 10% [16]. In order to distinguish the various possibilities, additional detailed investigations of the magnetoresistance in different current-field-axis geometries and neutron diffraction measurements on single crystals in magnetic fields would be helpful.

The additional peaks of the magnetoresistance, observed at low temperatures in the vicinity of the FOMPTs, are most likely initiated by reflections of a part of the conduction electrons from a potential barrier between the interphase boundary, separating phases with different magnetic structures. The width of the hysteresis loops, evaluated from the magnetoresistance data, obeys an activation-type behaviour at elevated temperatures. However, below about 0.6 K clear discrepancies from such a dependence occur which we attribute to a possible quantum tunnelling of magnetization. Of course, such a behaviour has to be proven by measurements at much lower temperatures than the present ones.

This work was in part supported by the Russian Foundation for Fundamental Research (Project 97-02-16504) and the Austrian FWF P12899.

References

1. E. Stryjewski, N. Giordano, Adv. Phys. **26**, 487 (1977).
2. N.V. Baranov, P.E. Markin, A.I. Kozlov, E.V. Sinitsyn, J. Alloys Comp. **200**, 43 (1993).
3. G.J. Primavesi, K.N.R. Taylor, J. Phys. F **2**, 761 (1972).
4. N.V. Baranov, A.N. Pirogov, A.E. Teplykh, J. Alloys Comp. **226**, 70 (1995).
5. H. Hirchmayr, E. Burzo, in *Landolt-Börnstein, Newseries, Group III, Vol. 19(d2)*, edited by H.P. Wijn (Springer-Verlag, Berlin, Heidelberg, New York, London, Paris, Tokyo, Hong Kong, Barcelona, 1990), pp. 1 ff.
6. J.S. Dugdale, *The electrical properties of metals and alloys* (Edward Arnold, London, 1977).
7. R.J. Elliot, F.A. Wedgwood, Proc. Phys. Soc. **81**, 846 (1963).
8. Y. Aoki, Y. Kobayashi, H. Sato, H. Sugawara, V. Sechovsky, L. Havela, K. Prokes, M. Mihalik, A. Menovsky, J. Phys. Soc. Jpn **65**, 3312 (1996).
9. R.B. Van Dover, E.M. Gyorgy, R.J. Cava, J.J. Krajewsky, R.J. Felder, W.F. Peck, Phys. Rev. B **47**, 6134 (1993).
10. N.V. Baranov, E.A. Barabanova, J. Alloys Comp. **219**, 139 (1995).
11. J.M. Ziman, *The electrons and phonons. Theory of transport phenomena in solids* (Oxford at the Clarendon Press, 1960).
12. N.V. Baranov, A.V. Andreev, A.I. Kozlov, G.M. Kvashnin, H. Nakotte, H. Aruga-Katori, T. Goto, J. Alloys Comp. **202**, 215 (1993).
13. O.V. Lounasmaa, R.A. Guenther, Phys. Rev. B **126**, 1357 (1962).
14. H. Yamada, S. Takada, Progr. Theoret. Phys. **49**, 1401 (1973).
15. T. Egami, Phys. Stat. Sol. A **19**, 747 (1973).
16. L.T. Rayevskaya, Sh.Sh. Abelskii, Yu.P. Irkhin, Solid State Phys. **20**, 1928 (1978).